Saddle-node ghost induced low-frequency fluctuations in an external-cavity laser diode

F. Rogister[1], P. Mégret, and M. Blondel

Service d'Electromagnetisme et de Telecommunications, Faculte Polytechnique de Mons
31 Boulevard Dolez, 7000 Mons, Belgium

We investigate the dynamics of a semiconductor laser subject to optical feedback and operating in the low-frequency fluctuation regime. We demonstrate that saddle-node ghosts can initiate the intensity dropouts that characterize this regime.

1. Introduction

When a laser diode is subjected to an external optical feedback and pumped close to its solitary threshold, its optical power can exhibit sudden dropouts that occur aperiodically. The typical duration between two consecutive dropouts is much larger than the period of the relaxation oscillations or the external-cavity round trip time. For this reason, this regime is usually referred to as the low-frequency fluctuation (LFF) regime. A widely accepted interpretation of this phenomenon was presented by Sano [1] in 1994; it relies on the Lang-Kobayashi equations [2] that assume single-mode operation of the laser and weak to moderate amount of external optical feedback. Sano showed that the intensity dropouts are caused by crises between local chaotic attractors and saddle-type antimodes.

In this article, we investigate the dynamics of a semiconductor laser pumped close to its solitary threshold and subject to two optical feedbacks. The increase of one of the feedbacks rate leads to the destruction of pairs of steady state solutions. However, even when they have disappeared, the fixed points continue to influence the dynamics of the system. We demonstrate for the first time that these saddle-node ghosts can initiate the intensity dropouts that characterize the low-frequency fluctuation regime.

2. Model and steady-state solutions

The Lang-Kobayashi equations [2] can be extended to the problem of a laser diode subject to optical feedback from a double cavity by including a second delay term in the rate equation for the electric field:

$$\frac{dE}{ds} = (1+i\alpha)NE + \kappa_1 E(s-\tau_1)\exp(-i\Omega\tau_1) + \kappa_2 E(s-\tau_2)\exp(-i\Omega\tau_2), \qquad (1)$$

$$T\frac{dN}{ds} = P - N - (1+2N)\,|E|^2. \qquad (2)$$

The dimensionless time s is measured in units of the photon lifetime τ_p; $E(s) = A(s)\exp[i\phi(s)]$ and $N(s)$ are the normalized slowly varying complex electric field and the normalized excess carrier number. κ_1 and κ_2 are the normalized feedback rates of the first and second external cavities and τ_1 and τ_2 the ratios of the round-trip time to the photon lifetime for those cavities. α is the linewidth enhancement factor and Ω is the product of the angular frequency of the solitary laser and the photon lifetime. P is the

[1] Electronic address: rogister@telecom.fpms.ac.be

dimensionless pumping current above solitary laser threshold and T the ratio of the carrier lifetime to the photon lifetime.

The steady-state solutions of Eqs. (1) and (2) can be written in the form

$$E = A_s \exp[i(\Delta - \Omega)s] \tag{3}$$

where Δ is the stationary angular frequency, A_s the amplitude and N_s the normalized carrier number. The stationary frequencies satisfy the equation

$$\Delta = \Omega - \kappa_1[\alpha\cos(\Delta\tau_1) + \sin(\Delta\tau_1)] - \kappa_2[\alpha\cos(\Delta\tau_2) + \sin(\Delta\tau_2)], \tag{4}$$

The results that we present here have been calculated for $\alpha = 4$, $T = 1000$, $\kappa_1 = 7.2 \times 10^{-3}$, $\tau_1 = 1400$, $\tau_2 = 1267 + 1.5\ \lambda/(2c\tau_p)$ where $\tau_p = 1$ps is the photon lifetime and c the velocity of light in vacuum. We assume that the laser works at the wavelength $\lambda = 780$ nm. For these numerical values, the phase-differences over one roundtrip in the first and the second cavities are approximately $\Omega\tau_1 \cong -2.90 \bmod 2\pi$ and $\Omega\tau_1 \cong 2.78 \bmod 2\pi$, respectively. In the following, κ_2 is the only variable parameter.

Similarly to the single-feedback case, the steady-state solutions are of two kinds: saddle points that we refer to as antimodes and other solutions that can be stable and that we call external cavity modes (ECM).

3. Numerical results

In this section, the temporal evolution of the intensity $|E|^2$ (Fig. 1) and the system trajectories in the plane $[\phi(t)\text{-}\phi(t\text{-}\tau_1)+\Omega\tau_1, N(t)]$ (Figs. 2 and 3) are calculated by solving numerically Eqs. (1) and (2). In Figs. 2 and 3, circles and squares represent ECMs and antimodes, respectively. When the first cavity is acting alone, i.e. $\kappa_2 = 0$, the trajectory displays chaotic itinerancy among seven attractor ruins of external cavity modes and collisions with three different antimodes [Fig. 2(a)]. Sharp intensity dropouts are clearly visible in Fig. 1(a). For $\kappa_2 = 1.2 \times 10^{-4}$, the ECM with the lowest frequency and the corresponding antimode collide and disappear through a saddle-node bifurcation. The LFF continues however [Fig. 1(b)], because crises with remaining antimodes still occur [Fig. 2(b)]. As κ_2 increases further, the ruin of the chaotic attractor associated to the lowest frequency external-cavity mode decreases progressively in size. For $\kappa_2 = 2.6 \times 10^{-4}$, the attractor does no longer collide with the saddle-point. Chaotic, quasiperiodic and periodic behaviors are successively observed from $\kappa_2 = 2.6 \times 10^{-4}$, to 8.4×10^{-4}. As an example, a stable chaotic attractor and a limit cycle are shown in Figs. 2(c) and (d) for $\kappa_2 = 2.8 \times 10^{-4}$ and $\kappa_2 = 4.5 \times 10^{-4}$, respectively. At $\kappa_2 = 8.4 \times 10^{-4}$, the lowest frequency ECM becomes stable through a Hopf bifurcation. From $\kappa_2 = 8.4 \times 10^{-4}$ to 1.34×10^{-3}, all trajectories are attracted by this stable points regardless of the initial conditions. As κ_2 increases, the ECM and the antimode come close to each other and finally collide at $\kappa_2 = 1.34 \times 10^{-3}$ and disappear. Fig. 3(a) shows the steady state solutions just before the saddle-node bifurcation. As this pair of steady state solutions disappears, an atypical LFF is observed: the trajectory in phase space exhibits a chaotic itinerancy among the external-cavity modes with a drift toward the lowest frequencies. The fixed points that have disappeared at $\kappa_2 = 1.34 \times 10^{-3}$ continue to influence the dynamics: they leave a ghost that attracts the trajectory. The trajectory is then repelled toward higher values of the excess carrier number along the direction of the unstable

manifold of the antimode that has disappeared [Fig. 3(b)]. As a result, the laser exhibits strong intensity dropouts that are not associated to attractor crises. Additional increase of κ_2 leads to a progressive attenuation of the influence of the annihilated fixed points on the dynamics as well as to a decrease in size of the ruin of the nearest chaotic attractor. Chaotic [Fig. 3(c)], quasiperiodic and periodic [Fig. 3(d)] behaviors are successively observed. Finally, at $\kappa_2 = 4.8 \times 10^{-3}$ the laser output becomes stationary. For $\kappa_2 \geq 4.8 \times 10^{-3}$, the rest of the bifurcation diagram reveals a scenario similar to that described in Refs [3] and [4], i.e. a succession of regions within which the laser is locked onto a stable maximum gain mode and regions where the laser exhibits complex behaviors such as chaos and low-frequency fluctuations.

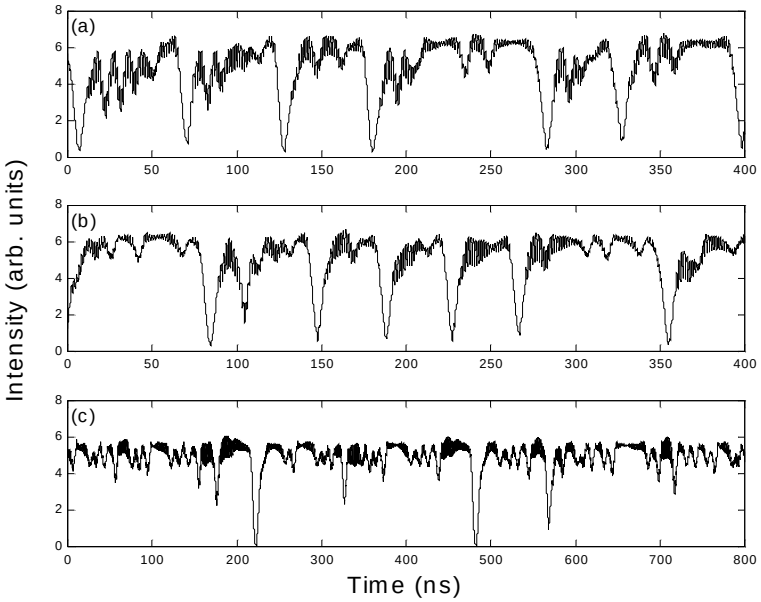

Figure 1

4. Conclusion

We have investigated the dynamics of a laser diode subject to optical feedback from a double cavity and pumped close to its solitary threshold. When both cavities are acting in concert, an increase of one of the feedback rate can lead to the annihilations of fixed points through saddle-node bifurcations. We have shown that the saddle-node remnants continue to influence the dynamics and can induce intensity dropouts. This kind of solution have not been reported so far in the extensively studied single feedback case. We attribute the difficulty to observe such dynamics in a single feedback system to the fact that, in this system, an increase of the feedback rate does never lead to the annihilation of fixed points.

This research was supported by the InterUniversity Attraction Pole (IAP V/18) program of the Belgian government. F. Rogister is a Scientific Research Worker of the Fonds National de la Recherche Scientifique (FNRS).

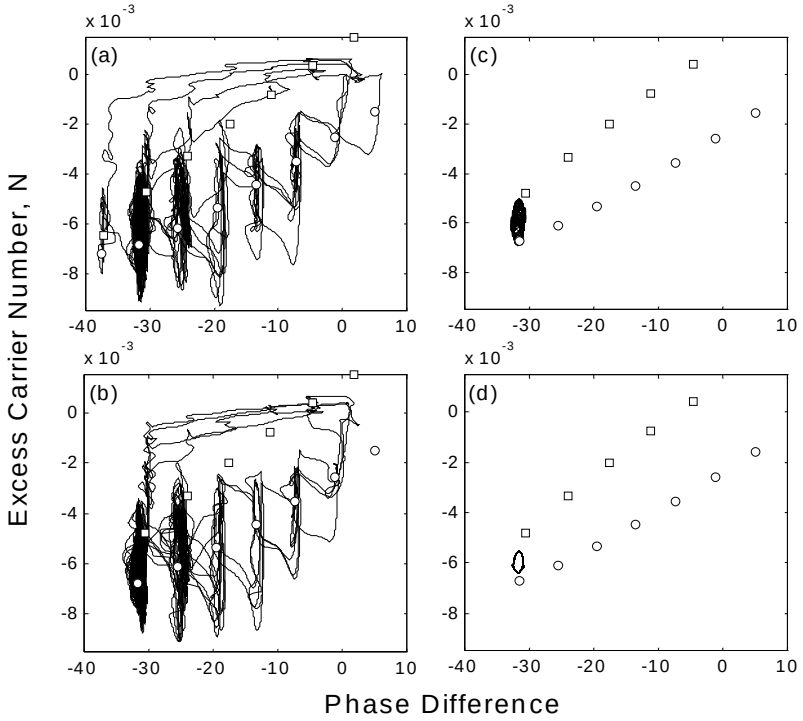

Figure 2

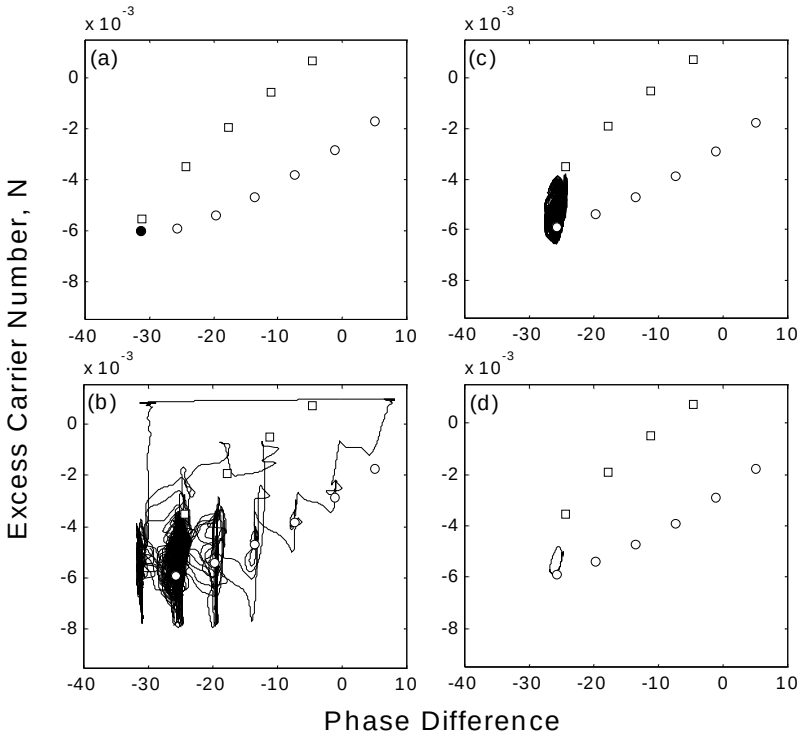

Figure 3

References

[1] T. Sano, Phys. Rev. A **50**, 2719 (1994).

[2] R. Lang and K. Kobayashi, IEEE J. Quant. Electr. **QE-16**, 347 (1980).

[3] F. Rogister, P. Mégret, O. Deparis, M. Blondel and T. Erneux, Opt. Lett. **24**, 1218 (1999).

[4] F. Rogister, D.W. Sukow, A. Gavrielides, P. Mégret, O. Deparis, and M. Blondel, Opt. Lett. **25**, 808 (2000).